Cellular and Molecular Neurobiology
https://doi.org/10.1007/s10571-022-01252-1

ORIGINAL RESEARCH

The Circadian Clock of Polarized Microglia and Its Interaction with Mouse Brain Oscillators

Petra Honzlová[1,2] · **Kateryna Semenovykh**[1] · **Alena Sumová**[1]

Received: 25 March 2022 / Accepted: 28 June 2022

Abstract

The activity of the immune system is controlled by circadian clocks present in different immune cells. The brain-resident subtype of immune cells, microglia, exhibits a wide range of functional phenotypes depending on the signaling molecules in their microenvironment. The exact role of microglia in the hypothalamic suprachiasmatic nuclei (SCN), the central circadian clock, has not been known. Therefore, the aim of this study was to determine (1) whether microenvironment-induced changes in microglial polarization affect circadian clocks in these cells and (2) whether the presence of microglia contributes to SCN clock function. Microglial and SCN clocks were monitored using PER2-driven bioluminescence rhythms at the tissue and single-cell levels. We found that polarization of resting microglia to a pro-inflammatory (M1) or anti-inflammatory (M2) state significantly altered the period and amplitude of their molecular circadian clock; importantly, the parameters changed plastically with the repolarization of microglia. This effect was reflected in specific modulations of the expression profiles of individual clock genes in the polarized microglia. Depletion of microglia significantly reduced the amplitude of the SCN clock, and co-cultivation of the SCN explants with M2-polarized microglia specifically improved the amplitude of the SCN clock. These results demonstrate that the presence of M2-polarized microglia has beneficial effects on SCN clock function. Our results provide new insight into the mutual interaction between immune and circadian systems in the brain.

Keywords Microglia · Polarization · Circadian clock · Suprachiasmatic nuclei · mPER2Luc mouse · PLX3397

Introduction

Microglia are phagocytes originating from myeloid precursors present in the embryonic yolk sac from where they migrate into the central nervous system (CNS) during prenatal development (Takahashi et al. 1989). In the CNS they represent approximately 10% of all cells (Lawson et al. 1992). They interact with a wide range of other cell types, such as neurons (Biber et al. 2007; Szepesi et al. 2018), astrocytes (Matejuk and Ransohoff 2020), or oligodendrocytes (Peferoen et al. 2014), and they are the first line of defense against injury and pathogens. Similar to macrophages, microglia exhibit a scale of functional phenotypes (Durafourt et al. 2012; Hu et al. 2014; Orihuela et al. 2016). As opposed to their original description, the so-called "resting" (M0) microglia represent a dynamic surveillance system responsible for homeostasis maintenance, regulation of synaptic organization, and debris removal (Davalos et al. 2005; Kabba et al. 2018). Classically activated or "M1" phenotype of microglia is induced upon injury or infection, and their role is to mediate the inflammatory reaction. Microglia polarize to M1 in response to pro-inflammatory stimuli, such as LPS and IFNγ, which determine their main role in destroying the invading pathogens. The process of inflammation is accompanied by increased release of inflammation-related cytokines (IL-1, IL-6, TNFα) or chemokines (CCL2) and induced reactive oxygen species (ROS) and NO production, which also has neurotoxic side effects (Durafourt et al. 2012; Tang and Le 2016; Orihuela et al. 2016). Alternatively activated "M2" microglia partake during the inflammation resolution process. M2-polarized state is induced by anti-inflammatory signaling molecules, i.e., IL-4, IL-10, IL-13, or glucocorticoids. M2 microglia then clear cellular debris through phagocytosis and release

✉ Petra Honzlová
petra.honzlova@gmail.com

[1] Laboratory of Biological Rhythms, Institute of Physiology, The Czech Academy of Sciences, Videnska 1083, Prague, Czech Republic

[2] Faculty of Science, Charles University, Prague, Czech Republic

Published online: 11 July 2022

neuroprotective and trophic factors, i.e., TGF-β or IGF-1, to promote axonal remodeling, neural repair, and neurovascular network restoration (Durafourt et al. 2012; Cherry et al. 2014; Hu et al. 2014; Orihuela et al. 2016). The properly timed transition between these microglia phenotypes is an essential condition for efficient healing of neural tissue after spinal cord or brain injury, brain ischemia, or acute neural tissue inflammation (Cherry et al. 2014; Li et al. 2017). If the process is uncontrolled, M1-induced inflammation could transit to its chronic form and contribute to the development of neurodegenerative diseases, such as Alzheimer's (Blasko et al. 2004) or Parkinson's (Son et al. 2008).

Microglia are, similar to other cells of the immune system, such as B cells, T cells, monocytes, and macrophages, also equipped with an oscillatory mechanism to serve as the peripheral clock of the circadian system (Bollinger et al. 2011; Silver et al. 2012; Chi-Castañeda and Ortega 2016). In mammals, these clocks are subordinated to the central clock residing within the suprachiasmatic nuclei (SCN) in the hypothalamus (Scheiermann et al. 2013). The SCN clock integrates information about environmental changes in light and darkness and synchronizes peripheral oscillators via neuronal (Bartness et al. 2001; Oster et al. 2006), humoral (Yamamoto et al. 2005; Pevet and Challet 2011), and other entraining signals (Bollinger and Schibler 2014). On the cellular level, the circadian clock operates via a mechanism based on transcription–translation feedback loops (TTFL) that result in rhythmic changes in expression levels of so-called "clock genes", namely *Clock*, *Bmal1* (*Arntl*), *Per1/Per2*, *Cry1/Cry2*, and *Nr1d1*(*Rev-erbα*) with a period close to 24 h (reviewed in Partch et al. 2014). Their protein products serve as transcription factors that regulate the expression of clock-controlled genes involved in various processes regarding cellular physiology and function (Bollinger and Schibler 2014). In microglia, the circadian clock drives several aspects of microglial physiology, including temporal morphology variations (Hayashi 2013), the rhythmic release of IL-1, TNFα, and IL-6 (Fonken et al. 2015; Nakazato et al. 2017), regulation of phagocytosis, or daily variations in the expression of genes related to nutrients utilization, glucose transportation, and oxidative stress protection (Wang et al. 2020). Additionally, microglia's response to LPS stimulation, such as induction of IL-1 and TNFα expression, is time-of-day dependent (Fonken et al. 2015).

Recently, the circadian clocks in differently polarized macrophages and the changes in their properties depending on their polarization state were studied (Chen et al. 2020; Timmons et al. 2020; Cui et al. 2021). Although peripheral macrophages share similar properties or characteristic markers (CD11b, F4/80) with microglia (Greter and Merad 2013), the fact that they differ in their origin (Prinz and Priller 2014), physiology (Kettenmann et al. 1990; Greenhalgh and David 2014), and even time-dependent immune responses (reviewed in Martínez-Tapia et al. 2020) justifies the need to consider them separately in research. Therefore, this study is the first to provide a comprehensive characterization of the circadian clock in differentially polarized microglia. In addition, it was aimed at demonstrating whether and how microglia polarization affects the robustness of the central circadian oscillator.

Materials and Methods

Animals

Transgenic PER2::LUC knock-in C57BL/6 J mice (Yoo et al. 2004) bred at the animal facility of the Institute of Physiology, CAS, were used for isolation and cultivation of microglia primary cell cultures and preparation of organotypic SCN explants.

The Animal Care and Use Committee of the Institute of Physiology, in agreement with the Animal Protection Law of the Czech Republic as well as European Community Council directives 86/609/EEC, approved all experiments. All efforts were made to alleviate the suffering of the animals.

Microglia Cultivation and Treatments

Mixed glial cultures were isolated from brains of 5 to 8-day-old mice. Mice were rapidly decapitated, and brains were removed and homogenized. Cell suspension was seeded for cultivation in DMEM high-glucose medium (Merck, D6546), 10% fetal bovine serum (Merck), 1% penicillin/streptomycin (Merck), and 1% Glutamax (Gibco). When the culture in the flask reached approx. 90% confluence, medium conditioned by L929 cell line (Tomida et al. 1984) was added to the cultivation medium (30%) for 5 days. Cells were then detached from culture by shaking (180 rpm, 1.5 h, 37 °C), and microglia were selectively isolated via magnetic separation using CD11b Microbeads (Miltenyi Biotec) according to manufacturer's instructions and seeded for further experiments.

Microglia were seeded 50,000 cells/sample and left for 2 days to attach to the surface. Microglia were synchronized using serum shock (50% horse serum, 2 h, 37 °C) and transferred into an air-buffered recording medium (Yamazaki and Takahashi 2005) supplemented with 10% fetal bovine serum (Merck), 1% Glutamax (Thermo Fisher Scientific), 0.1% Gentamycin (Merck), and 0.1 mM CycLuc1 substrate (Merck).

Air-buffered bioluminescence recording medium either remained untreated (M0 polarization), or it was enriched by LPS (50 ng/ml; Invitrogen) and IFNγ (20 ng/ml; Peprotech) to induce M1 polarization or IL-4 (20 ng/ml; Peprotech) to induce M2 polarization.

SCN Isolations and Treatments

SCN organotypic explants were prepared as previously described (Sládek and Sumová 2019). Briefly, the mice were sacrificed via rapid cervical dislocation, and hypothalamic regions containing the SCN were sliced on a vibratome (VT1200S, Leica, two 250 µm slices/mouse). The explants were immediately placed onto Millicell Culture Inserts (Merck) inside 35 mm Petri dishes with 1 ml of air-buffered recording medium supplemented with 100 U/ml penicillin, 100 µg/ml streptomycin, 1 × GlutaMAX (Thermo Fisher Scientific), 2% B27 supplement (Thermo Fisher Scientific), and 0.1 mM D-Luciferin (Biosynth).

To deplete resident microglia within the explant, PLX3397 (1 µM, Merck) or vehicle (VEH_{PLX}; 0.01% DMSO) was added to the medium for at least 10 days. SCN were further treated with TNFα (20 ng/ml; Peprotech), IL-6 (10 ng/ml; Peprotech), IL-1 (5 ng/ml; Peprotech), IFNγ (20 ng/ml; Peprotech), LPS (50 ng/ml; Invitrogen), or IL-4 (20 ng/ml; Peprotech). To avoid phase-dependent variation in clock reactions, SCN were treated with cytokines, endotoxin, and their respective vehicles at the same phase.

Bioluminescence Monitoring

SCN organotypic explants were recorded in the LumiCycle apparatus (Actimetrics) and the raw bioluminescence traces were analyzed using the LumiCycle Analysis software (Actimetrics). Bioluminescence in microglia cell cultures was recorded using the Luminoskan Ascent apparatus (Thermo Fisher Scientific). Recorded traces were analyzed using adapted (https://github.com/clockgene/per2py_luminoskan) Python script "per2py" (https://github.com/johnabel/per2py) for automated analysis of circadian bioluminescence data (Li et al. 2020). Relative amplitude was calculated relative to values from M0 microglia. To calculate gradual damping of amplitude over time, on each detrended trace the amplitude of the first five peaks was measured and then normalized to the highest one.

On a single-cell level, microglia were recorded in a motorized Luminoview LV200 luminescence microscope (Olympus) with LUCPLFLN40X objective (Olympus) and an ImageEM X2 EMCCD camera (Hamamatsu) water-cooled by a Minichiller 280 (Huber) with an exposure time of 60 min. Background noise and cosmic rays were removed using a median filter. Individual cells were outlined and tracked using the Trackmate (Tinevez et al. 2017) plugin in ImageJ/Fiji software (Schindelin et al. 2012). Traces longer than 48 h were then analyzed using an adapted "per2py" script (https://github.com/clockgene/per2py_trackmate).

Viability Test

Viability and innate metabolic activity were assessed using Resazurin assay (Rampersad 2012) according to the manufacturer's instructions. Resazurin (Sigma-Aldrich) was added to synchronized and polarized microglia in an air-buffered recording medium right away (0 h) or 96 h after polarization. After 3 h medium was collected and absorbance was measured on Infinite M200 Reader (Tecan Life Sciences). For each sample, absorbance percentage reduction is calculated using the following equation: Resazurin reduction percentage = $[(\varepsilon OX_{600nm} \times A_{570nm\_t3} - \varepsilon OX_{570nm} \times A_{600nm\_t3})/(\varepsilon RED_{570nm} \times A_{600nm\_nc} - \varepsilon RED_{600nm} \times A_{570nm\_nc})] \times 100$. εOX represents the molar extinction coefficient of oxidized Resazurin at 570 nm/600 nm, εRED represents the molar extinction coefficient of reduced Resazurin at 570 nm/600 nm, and A is the measured absorbance at 570 nm/600 nm of negative control (nc) and after 3 h of incubation (t3).

Daily Profiles of Gene Expression

Microglia were seeded (100,000 cells/sample), left undisturbed for two days to adhere to the surface, synchronized using serum shock (as described above), and polarized in the cultivation medium. Then, 24 h after polarization, microglia samples were collected every 4 h over 24-h interval for detection of expression profiles, five samples per time point. RNA was isolated using the RNeasy Micro kit (Qiagen) according to the manufacturer's instructions. RNA samples were reverse transcribed into cDNA using the High-Capacity cDNA Reverse Transcription Kit (Applied Biosystems). The cDNA samples were analyzed by real-time PCR using PowerUp SYBR Green Master Mix (Applied Biosystems) on a ViiA7 Real-Time PCR System (Life Technologies). For specific primers, see Table 1. The ΔΔCt method was used for the quantification of relative cDNA concentration. Relative expression was achieved by normalizing the expression to the mean relative expression of the hypoxanthine-guanine phosphoribosyltransferase (*Hprt*) housekeeping gene. For analysis of culture purity, relative gene expression of microglia (*Aif1*, also known as *Iba1*) and astrocyte (*Gfap*) markers was assessed for all samples of all three polarizations and all time points pooled together. For analysis of gene expression levels of polarization markers (*Arg1*, *Nos2*), results were pooled together from all time points for each polarization.

Western Blot

Organotypic explants of SCN were pooled (3 explants per sample) and lysed in 50 µl of ice-cold RIPA buffer supplemented with protease and phosphatase inhibitors. Lysates were heated for 10 min at 70 °C with LDS Sample buffer

Table 1 Primers

Hprt	F-AGGGATTTGAATCACGTTTG
	R-TTTACTGGCAACATCAACAG
Per2	F-CTTTCACTGTAAGAAGGACG
	R-CTGAGTGAAAGAATCTAAGCC
Arntl (Bmal1)	F-GCAAGAAGATTCTAAATGGAGG
	R-GGTTCTCACCAAGAATAGAAG
Clock	F-CCTCAGGCACGTGAAAGAAAAG
	R-GCAAGGCCGTCTTCTGTGTG
Nr1d1	F-AACATTACCAAGCTGAATGG
	R-CTGGATATTCTGTTGGATGC
Cry1	F-AGAAGGGATGAAGGTCTTTG
	R-CTCTTAGGACAGGTAAATAACG
Arg1	F-CTGACCTATGTGTCATTTGG
	R-CATCTGGGAACTTTCCTTTC
Nos2	F-CATCAACCAGTATTATGGCTC
	R-TTTCCTTTGTTACAGCTTCC
Aif1 (Iba1)	F-TTCATCCTCTCTCTTCCATC
	R-TCAGCTTTTGAAATCTCCTC
Gfap	F-GGAAGATCTATGAGGAGGAAG
	R-CTGCAAACTTAGACCGATAC
Pparg	F-AAAGACAACGGACAAATCAC
	R-GGGATATTTTTGGCATACTCTG

List of forward and reverse primers used for gene expression analysis

(Thermo Fisher Scientific) and dithiothreitol, then separated using Bolt 4–12%, Bis–Tris Mini Protein Gel (Thermo Fisher Scientific) in MOPS buffer (Thermo Fisher Scientific) according to the manufacturer's instructions, and transferred onto a nitrocellulose membrane. After blocking, the membrane was split at approximately 30 kDa and proteins were separately labeled overnight at 4 °C with rabbit IBA1 antibody (1:1000, 019-19741, Wako) and with anti-actin antibody (1:4000, A2066, Merck) as a loading control. Membranes were then incubated with HRP-conjugated anti-rabbit antibody (1:10,000, Merck) for 1 h. After short incubation with the substrate (SuperSignal West Femto Maximum Sensitivity Substrate, Thermo Fisher Scientific), membranes were scanned using ChemiDoc System (Biorad). Obtained images were analyzed in ImageLab 6.0 software (Biorad). Relative volume was normalized to a sample of microglia (referred to as PC, positive control) isolated from cell culture as described above (250,000 cells/50 µl RIPA buffer) present on the membrane.

Statistical Analysis

Relative expression of microglia and astrocyte marker genes, results of resazurin viability assay (for each polarization separately), and relative changes in period and amplitude of SCN-generated rhythms were compared using unpaired t tests. Changes in period length after polarization change were analyzed using paired t tests.

Relative expression of polarization marker genes and bioluminescence rhythms' parameters on both culture and single-cell levels were analyzed using one-way ANOVA followed by the post hoc analysis with Sidak's multiple comparison method.

Comparison of amplitude damping rate over time and differences in daily profiles of gene expression were assessed using two-way ANOVA followed by the post hoc analyses with Sidak's multiple comparison method.

Daily profiles of gene expression were analyzed by cosinor analysis for detection of the presence/absence of a circadian rhythm as previously described (Sládek et al. 2012). Briefly, two alternative regression models were compared to fit the data: a horizontal straight line (null hypothesis) or a single cosine curve (alternative hypothesis), defined by the equation $Y = \text{mesor} + [\text{amplitude} \times \cos(2 \times \pi \times (\text{X-acrophase})/\text{wavelength})]$ with a constant wavelength of 24 h, to differentiate between non-rhythmic and rhythmic expression, respectively. The extra sum-of-squares F test was used for comparison, and the cosine curve parameters were calculated unless the *P*-value exceeded 0.05. For comparison, the amplitudes and mesors were normalized relative to the value of the M0 group and compared by one-way ANOVA followed by the post hoc analysis with Sidak's multiple comparison method (Novosadová et al. 2018).

All statistics were performed using Prism 7 software (GraphPad). $P < 0.05$ was required for significance.

Results

Microglia's Polarization Affects Properties of Their Circadian Clock

$CD11b^+$ microglia were isolated from mixed glial primary cultures derived from brain tissue of PER2::LUC knock-in mice. The purity of $CD11b^+$ microglia cultures was checked by analysis of gene expression of microglia-specific marker *Iba1 (Aif1)* to exclude the contamination with astrocytes, which on their own also generate circadian rhythms (Prolo et al. 2005). In the cultures, *Iba1* was significantly upregulated ($P < 0.0001$) compared to very low or undetectable expression of astrocyte-specific *Gfap* (Fig. 1A).

After serum shock-induced synchronization, microglia cultures either remained untreated to represent the "resting" (M0) phenotype or they were polarized to M1 (treated with LPS and IFNγ) or M2 (treated with IL-4) state. Polarization was confirmed by upregulated gene expression levels of M1- and M2-specific polarization markers *Nos2* (M0 vs. M1,

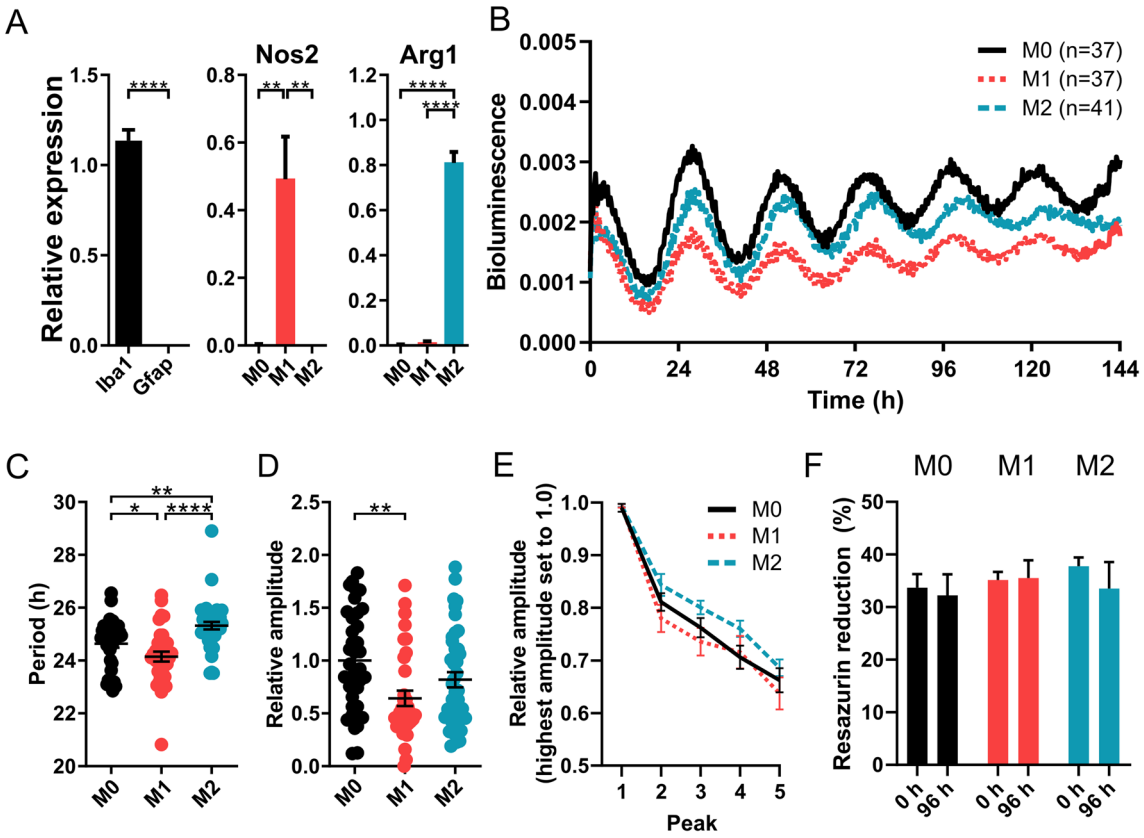

Fig.1 Distinct properties of the circadian clock in resting (M0)-, M1-, and M2-polarized microglia. **A** Relative expression of microglia and astrocyte-specific markers *Iba1* (*Aif1*) and *Gfap*, respectively, confirming the purity of isolated microglia cultures, and polarization-specific markers *Nos2* and *Arg1*, confirming successful polarization, **B** mean composite traces of bioluminescence rhythms in M0 (black full line)-, M1 (red-dotted line)-, and M2 (blue-dashed line)-polarized microglia ($n=37$–41), **C** period, **D** relative amplitude, and **E** gradual dampening of the amplitude of PER2-driven bioluminescence rhythms of M0 (black full line)-, M1 (red-dotted line)-, and M2 (blue-dashed line)-polarized microglia, **F** resazurin viability test performed on polarized microglia cultures immediately after synchronization (0 h) and after 96 h in cell culture. Data are expressed as mean ± SEM. $^{*}P<0.05$, $^{**}P<0.01$, $^{****}P<0.0001$

$P=0.0013$; M2 vs. M1, $P=0.0036$) and *Arg1* (M0 vs. M2, $P<0.0001$; M1 vs. M2, $P<0.0001$), respectively (Fig. 1A).

PER2-driven bioluminescence was monitored in the M0, M1, and M2 microglia cultures for approximately 6 days ($n=37$–41 each phenotype; mean composite traces from all samples are presented in Fig. 1B). Parameters of the recorded rhythms, namely period, relative amplitude, and gradual damping rate of amplitude, were analyzed (Fig. 1C-E).

Compared to "resting" (M0) microglia, clock in M1 microglia exhibited significantly shorter period (M0 vs. M1, $P=0.0345$), whereas M2 microglia-generated rhythms had significantly longer period (M0 vs. M2, $P=0.0049$; M2 vs. M1, $P<0.0001$; Fig. 1C). Although PER2-driven bioluminescence oscillations in M1 microglia had lower relative amplitude (M0 vs. M1, $P=0.0041$, Fig. 1D), the gradual damping of the rhythms (Fig. 1E) progressed similarly in all three polarized phenotypes. Resazurin-based viability test, which was performed at the beginning of cultivation (0 h) and after four days in culture (96 h), confirmed that survival of cells over time did not differ among the individual polarizations (M0: 0 h vs. 96 h, $P=0.7548$; M1: 0 h vs. 96 h, $P=0.9158$; M2: 0 h vs. 96 h, $P=0.4170$; Fig. 1F). Therefore, the differences in the clock properties between the polarized microglia cultures were not due to the different viabilities of the cell cultures.

Polarization Plastically Modulates the Period of the Microglia Circadian Clock

Microglia polarization is not an ultimate state as they need to plastically react to changing conditions within the CNS environment and adjust their functional phenotype accordingly. The question remains whether the properties of the microglial circadian clock reflect changes in their phenotype. Therefore, the microglia cultures were first polarized (M0 or M1) and recorded for 72 h. Thereafter, the original culture medium was removed, microglia were washed in PBS

for 10 min, and then they were cultured either in a medium of the same composition (groups M0 → M0 and M1 → M1) or in a medium containing either pro-inflammatory (LPS, IFNγ) or anti-inflammatory (IL-4) signaling molecules (groups M0 → M1 and M1 → M2, respectively) and recorded for additional 72 h. Mean composite traces of all recordings within each group ($n = 7–10$) are depicted in Fig. 2A. For each sample, the period of the PER2-driven bioluminescence rhythm was calculated before and after the medium change (Fig. 2B). The period did not significantly change in control groups that after wash remained in the medium of the same composition (M0 → M0, $P = 0.0693$; M1 → M1, $P = 0.4137$). On the other hand, prominent changes were detected in groups, where we simulated the switch from "resting" to pro-inflammatory polarized state (M0 → M1) and the transition from pro-inflammatory to anti-inflammatory phenotype (M1 → M2). The period of the circadian clock in microglia significantly shortened after stimulation with LPS and IFNγ (M0 → M1, $P = 0.0003$), whereas it significantly lengthened after stimulation with IL-4 (M1 → M2, $P = 0.0007$). The polarization-induced changes are in accordance with the results presented in Fig. 1C. Altogether, the results demonstrate that properties of the microglia circadian clock are not ultimately determined by the original exposure to polarizing agents. Instead, they are able to plastically react to changes in their microenvironment in accordance with the changes in microglia phenotype.

Polarization-Specific Properties of the Circadian Clock in Microglia are Detectable at the Level of Individual Cells

To further elaborate the findings, PER2-driven bioluminescence rhythms were recorded in individual-polarized microglia cells using bioluminescence microscopy. In the Supplement, bright field (Online Resource 1–3) and luminescence (Online Resource 4–6) recordings of polarized microglia are shown.

Individual cells (Fig. 3A) were tracked during the recording. Representative bioluminescence traces of single cells from the M0-, M1-, and M2-polarized cultures are shown in Fig. 3B. Parameters of the traces were analyzed (Fig. 3C; for details see Materials and Methods). Rhythms of M1-polarized microglia recorded at the single-cell level exhibited significantly shorter period (M0 vs. M1, $P = 0.0199$; M1 vs. M2, $P = 0.0077$) and decreased relative amplitude (M0

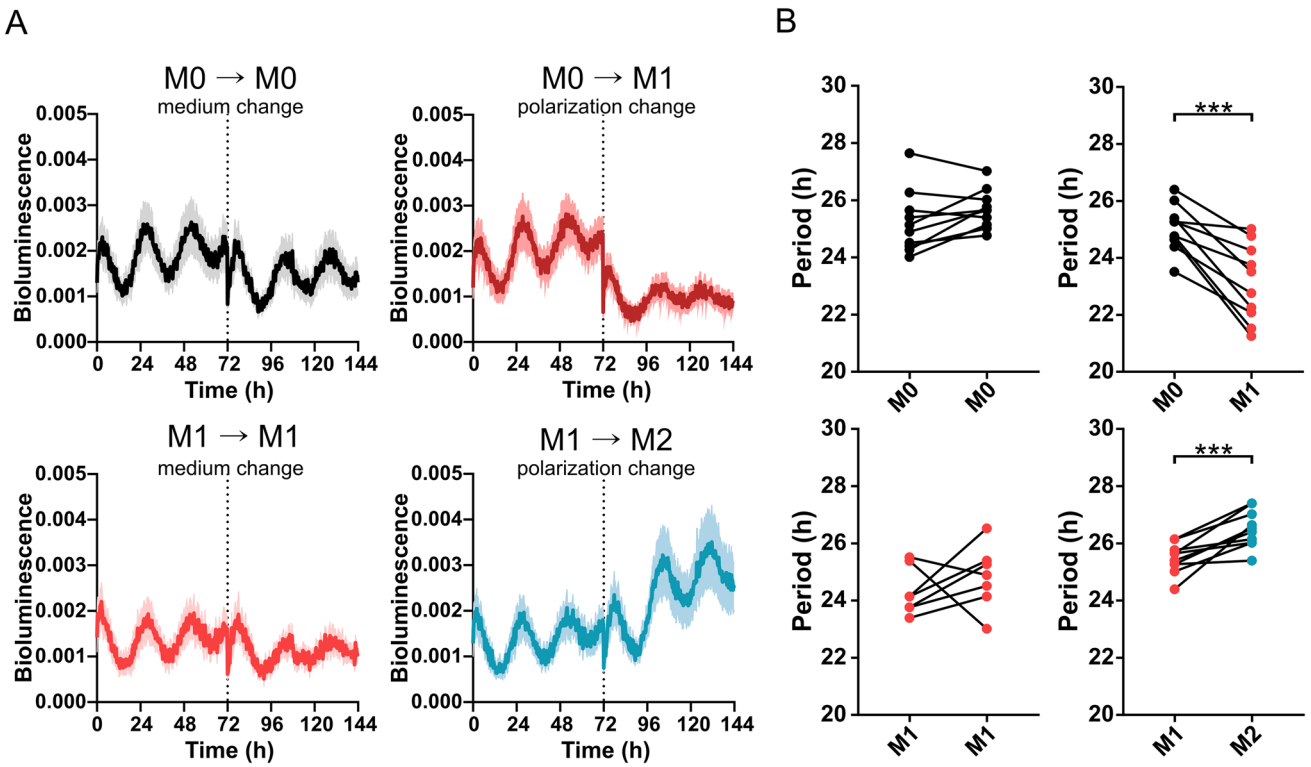

Fig.2 Circadian clock properties plastically react to polarization change in microglia. **A** Mean composite traces of bioluminescence rhythms ± SEM ($n = 7–10$). Microglia were polarized and recorded for 72 h. The cultivation medium was then washed out and microglia were transferred to a new medium. Microglia in control groups (M0 → M0 and M1 → M1) received a medium with the same composition. Microglia in M0 → M1 received a medium containing LPS and IFNγ upon wash and microglia in M1 → M2 received a medium containing IL-4 to induce polarization change, **B** period before and after polarization change. ***$P < 0.001$

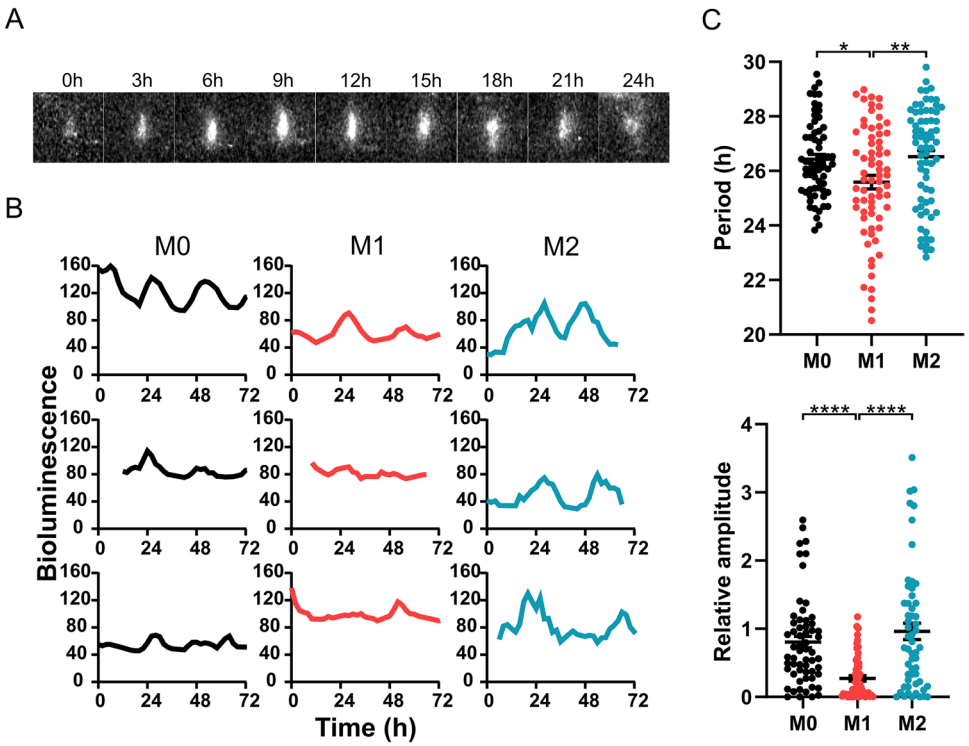

Fig.3 Bioluminescence recordings in individual-polarized microglia cells. **A** Illustrative time-lapse microscopy of individual microglia cell over 24 h, **B** representative bioluminescence traces recorded from individual cells of M0-, M1-, and M2-polarized microglia, **C** period and relative amplitude of analyzed rhythms. Data are expressed as mean ± SEM. $*P<0.05$, $**P<0.01$, $****P<0.0001$

vs. M1, $P<0.0001$; M1 vs. M2, $P<0.0001$; M0 vs. M2, $P=0.4108$) compared to M0 and M2 microglia. These results confirmed our observations from recordings on the cell culture level (Fig. 1C, D).

In contrary to the results shown in Fig. 1C, the period of M0- and M2-polarized microglia did not significantly differ (M0 vs. M2, $P=0.9586$), which might be partially attributed to a relatively large variance between the individual cells.

Polarization Alters Clock Gene Expression Profiles in Microglia Cultures

To assess the daily expression profiles of clock genes, samples of microglia cultures were first synchronized and polarized, left undisturbed for a full day, and then they were collected every 4 h to create a 24-h profile (Fig. 4A). The presence or absence of rhythmicity of the clock gene expression was assessed by the cosinor analysis (for details see Materials and Methods). Results of the analysis, as well as parameters of fitted sine curves, are summarized in Table 2.

Statistical comparisons of the parameters (Fig. 4B) are shown in Table 3. For *Clock* gene expression, the relative amplitude and mesor could not be compared between the experimental groups because rhythmicity was not confirmed in all polarizations; the rhythm was detected only in M2-polarized microglia. Significantly rhythmic expression was confirmed for all other studied clock genes (*Per2*, *Cry1*, *Bmal1*, and *Nr1d1*) in all three microglia polarizations.

Notably, the mean *Per2* expression level (mesor) was significantly decreased in M1-polarized microglia compared to M0 phenotype, which was in agreement with decreased amplitudes in PER2-driven bioluminescence recordings in vitro (Fig. 1 and Fig. 3). Additionally, the *Bmal1* mean expression level was decreased. Concurrently, M1 polarization substantially upregulated the expression of *Cry1* and *Nr1d1* and increased the amplitude of the *Nr1d1* rhythm. The mutual changes in expression levels are in accordance with the current TTFL model, i.e., participation of *Cry1* in the negative branch of the circadian clock's TTFL (inhibiting CLOCK/BMAL1-mediated *Per2* transcription) and of *Nr1d1* in repression of *Bmal1* expression. On the contrary, the polarization of microglia to M2 phenotype did not affect the amplitudes of the clock gene expression rhythms compared to M0 phenotype but mean expression levels were significantly upregulated for *Per2* and downregulated for *Bmal1*. M1 and M2 phenotypes differed in *Per2*, *Nr1d1*, and *Cry1* mean expression levels. Altogether, the results revealed that polarization significantly modulates the molecular mechanism of the microglia circadian clock.

Next, we explored the possibility that microglia clock can be regulated through PPARγ activation (Online Resource 7), which is closely related to the regulation of *Nr1d1* promoter (Kawai and Rosen 2010) and previously, the activity of nuclear receptor PPARγ was shown to modulate the polarization of microglia in favor of the anti-inflammatory M2 phenotype (Hu et al. 2014; Wen et al. 2018). The *Pparγ* expression differed between the

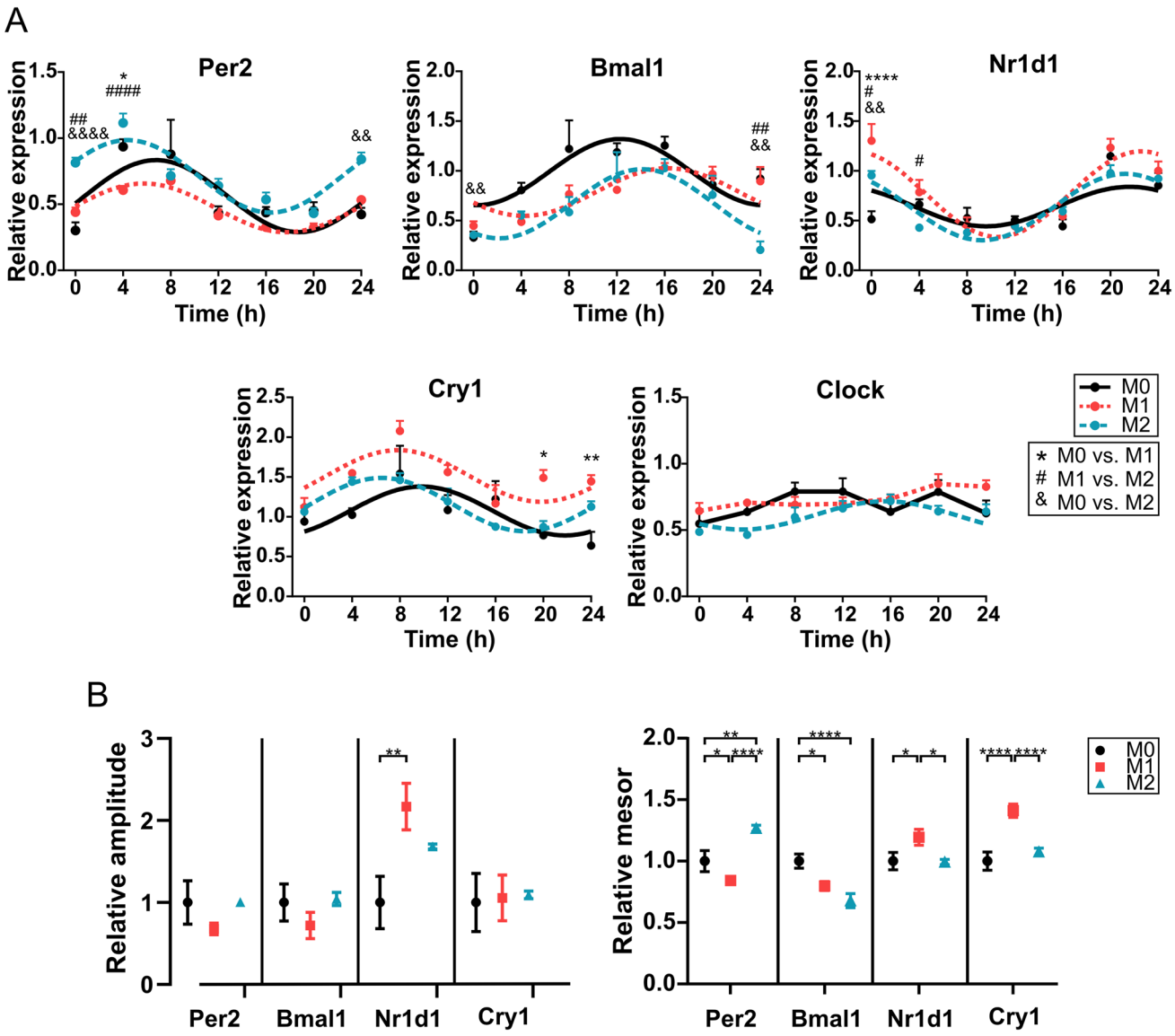

Fig.4 Daily clock gene expression profiles in polarized microglia. **A** 24-h profiles of relative gene expression of *Per2*, *Cry1*, *Bmal1*, *Cry1*, *Clock*, and *Nr1d1* in M0 (black circles, black full line), M1 (red circles, red-dotted line), and M2 (blue circles, blue-dashed line). Significant differences between groups at individual time points are depicted as indicated by two-way ANOVA post hoc analysis. M0 vs. M1: $^{*}P<0.05$, $^{**}P<0.01$; $^{****}P<0.0001$; M1 vs. M2: $^{\#}P<0.05$, $^{\#\#}P<0.01$; $^{\#\#\#\#}P<0.0001$; M0 vs. M2: $^{\&\&}P<0.01$, $^{\&\&\&\&}P<0.0001$. **B** Comparison of relative amplitudes and relative mesors of the cosine fits of rhythmic gene expression profiles in M0 (black circles), M1 (red squares), and M2 (blue triangles) depicted in (**A**) $^{*}P<0.05$, $^{**}P<0.01$, $^{****}P<0.0001$. Data are expressed as mean ± SEM

microglia polarizations; the levels were significantly downregulated in M1 and upregulated in M2. However, nuclear PPARγ protein levels were significantly higher in M0 compared to M1 and M2 microglia. Treatment of the M0, M1, and M2 microglia cultures with the PPARγ activator Rosiglitazone or PPARγ inhibitor GW9662 did not affect the period of the rhythms, except for Rosiglitazone shortening the period in M0 microglia where the levels of protein present in the nucleus were the highest. Therefore, activation of PPARγ affected the period of the circadian clock only in the microglia's resting state. All related data are presented in Supplemental Fig.S1 (Online Resource 7).

Microglia Depletion Affects Rhythmic PER2 Expression in SCN Explants

The impact of microglia depletion on maintenance of SCN-generated circadian rhythms was studied using in vitro SCN organotypic explants from PER2::LUC knock-in C57BL/6 J mice. SCN explants were cultivated for at least 10 days with

Table 2 Results of cosinor analysis of 24-h profiles of clock gene expression in polarized microglia

Gene	*Per2*	*Cry1*	*Bmal1*	*Nr1d1*	*Clock*
M0					
P-value	0.0027	0.0286	0.0005	0.0131	0.2244
Amplitude					
Mean	0.27	0.31	0.33	0.20	–
SEM	0.07	0.11	0.08	0.06	–
Mesor					
Mean	0.56	1.07	0.99	0.64	–
SEM	0.05	0.08	0.06	0.05	–
M1					
P-value	< 0.0001	0.0026	0.0004	< 0.0001	0.1745
Amplitude					
Mean	0.18	0.32	0.24	0.43	–
SEM	0.02	0.09	0.05	0.06	–
Mesor					
Mean	0.47	1.51	0.79	0.77	–
SEM	0.01	0.06	0.04	0.04	–
M2					
P-value	< 0.0001	< 0.0001	0.0006	< 0.0001	0.0023
Amplitude					
Mean	0.27	0.33	0.35	0.33	0.11
SEM	0.04	0.05	0.08	0.03	0.03
Mesor					
Mean	0.71	1.15	0.67	0.64	0.61
SEM	0.03	0.03	0.06	0.02	0.02

Rhythmicity of clock gene expression was determined using cosinor analysis (for details, see Materials and Methods "Statistical Analysis"). Expression was deemed as rhythmic unless *P*-value exceeded 0.05. If rhythmic, parameters of the best fit sine curve, namely amplitude and mesor, were calculated. SEM for each calculated parameter is included

CSF-1R inhibitor PLX3397, which was previously shown to effectively deplete neural tissue explants of resident microglia (Coleman et al. 2020). The effectiveness of the depletion was confirmed by a significant decrease in levels of IBA1 microglia marker in the SCN organotypic explants as detected by Western blot ($P = 0.0292$; Fig. 5A). In the explants treated with PLX3397 or vehicle (VEH_{PLX}), bioluminescence was recorded during this time (representative recordings are shown in Fig. 5B). The medium was refreshed for the explants after approximately 5 days in culture. To determine the effect of microglia depletion on the SCN clock, the relative change of period and amplitude was assessed as a difference between the parameters detected during the first (day 1–5) and the second half (day 6–11) of cultivation with PLX3397 or vehicle (Fig. 5C). Data show that depletion of microglia did not affect the period of the clock in the SCN ($P = 0.8118$), but it lead to an accelerated decrease in amplitude of SCN rhythms ($P = 0.0037$). PLX3397 treatment did not affect mean bioluminescence levels (Fig. 5C, $P = 0.1917$) which excluded the possibility that the observed effect was caused by PLX3397-induced impairment in explant viability.

Microglia Depletion Modulates Responses of the SCN Clock to LPS and TNFα

To explore how microglia activity regulates responses of the SCN clock to pro- and anti-inflammatory stimuli, bioluminescence of both intact (VEH_{PLX}) and microglia-depleted (PLX3397) SCN explants was recorded for two full circadian cycles before their treatment with an array of pro-inflammatory (TNFα, IL-6, IL-1, IFNγ, LPS) and anti-inflammatory (IL-4) signaling molecules. Relative changes in periods and amplitudes of the bioluminescence rhythms were calculated as their difference before and after treatment (Fig. 5D). Results are summarized in Table 4. Microglia depletion shortened the period of rhythm in TNFα-treated SCN explants and in explants treated with LPS, it decreased the amplitude of the rhythms.

M2-Polarized Microglia Increase Amplitude of the SCN Rhythmicity

Findings that the microglia presence affects the circadian clock in the SCN explants and its response to

Table 3 Results of one-way ANOVA comparison of clock gene expression rhythms in polarized microglia

Gene	Amplitude			Mesor		
	M0 vs. M1	M1 vs. M2	M0 vs. M2	M0 vs. M1	M1 vs. M2	M0 vs. M2
Per2	0.3790	0.9792	0.3790	0.0404	0.0013	< 0.0001
Bmal1	0.4343	0.8546	0.4343	0.0128	< 0,0001	0.1049
Nr1d1	0.0034	0.1036	0.1672	0.0411	0.9262	0.0411
Cry1	0.9926	0.9926	0.9926	< 0.0001	0.3398	< 0.0001
Clock	–	–	–	–	–	–

Parameters of best fit sine curve calculated by cosinor analysis, namely amplitude and mesor, were compared between groups of polarized microglia (M0, M1, and M2) for each clock gene. Parameters were not compared for *Clock*, as it was not deemed as rhythmic by cosinor analysis for all experimental groups

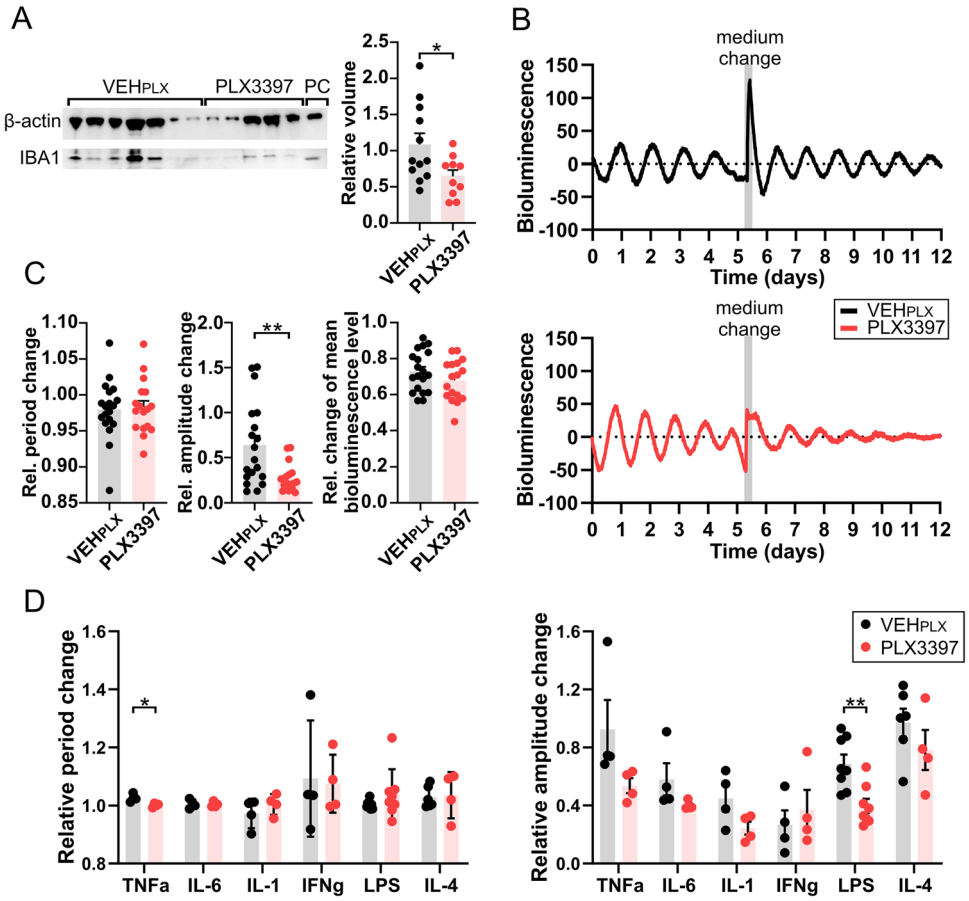

Fig.5 Effect of microglia depletion of SCN clock and its reaction to pro-inflammatory and anti-inflammatory signalization. SCN organotypic explants were incubated with CSF-1R inhibitor PLX3397 for at least 10 days to deplete them of microglia. **A** Comparison of levels of microglia marker IBA1 in SCN organotypic explants after 10-day treatment with PLX3397 or vehicle (VEH_{PLX}; 3 explants were pooled per sample) using Western blot. B-actin was used as a loading control, and the relative band volume of IBA1 was normalized to a positive control (PC, sample of microglia from primary cell culture), **B** bioluminescence recording of VEH_{PLX} (top, black line)- and PLX3397 (bottom, red line)-treated SCN explants (representative recordings), **C** relative change of period, amplitude and mean level of PER2-driven bioluminescence rhythms in VEH_{PLX}- and PLX3397-treated SCN explants, **D** PLX3397-treated SCN explants were treated with an array of pro-inflammatory and anti-inflammatory signaling molecules, namely TNFα, IL-6, IL-1, IFNγ, LPS, and IL-4. Relative change in period and amplitude before and after treatment were calculated. Data are expressed as mean ± SEM. $^{*}P < 0.05$, $^{**}P < 0.01$

pro-inflammatory signaling opened a question of how is the central oscillator affected by changes in polarization of the interacting microglia.

Microglia were isolated from primary cultures in the same way as in the previous experiments. Upon isolation of $CD11b^{+}$ cells, microglia were resuspended in an air-buffered recording medium used for the cultivation of SCN explants. M1 or M2 polarization was induced by adding LPS + IFNγ or IL-4 to the medium, respectively. Medium containing polarizing cytokines with or without microglia was then applied (in the total volume of 2 µl) on top of the organotypic SCN explants, which were pretreated with PLX3397. To avoid oversaturation of the explant with microglia, the number of microglia applied per SCN explant was approximated to 1500 cells/explant (Güldner 1983; Lawson et al. 1992).

Relative change of period and amplitude was calculated and compared between explants that were co-cultivated with and without primary culture microglia (Fig. 6A–C). Representative bioluminescence records for each group are depicted in Fig. 6D–F for co-cultivation with M0, M1, and M2 microglia, respectively.

Co-cultivation with M0 (Fig. 6A; relative period change: $P = 0.6476$; relative amplitude change: $P = 0.7739$) or M1 (Fig. 6B; relative period change: $P = 0.8136$; relative amplitude change: $P = 0.9407$)-polarized microglia had no effect on both rhythmic parameters (period, amplitude) of the central SCN clock. Co-cultivation with M2-polarized microglia also did not affect the period but significantly increased the amplitude of the SCN-generated oscillations (Fig. 6C; relative period change: $P = 0.6259$; relative amplitude change: $P = 0.0473$).

Table 4 Results of unpaired t test comparison of relative period and amplitude change in intact or microglia-depleted SCN explants after stimulation by pro-inflammatory or anti-inflammatory signaling molecules

Treatment	Rel. amplitude change (*P*-value)	Rel. period change (*P*-value)
TNFα	0.1122	0.0164
IL-6	0.1605	0.7545
IL-1	0.0907	0.3555
IFNγ	0.5643	0.8787
LPS	0.0056	0.2534
IL-4	0.2812	0.8491

Changes in parameters of PER2-driven bioluminescence rhythms before and after treatment with an array of pro-inflammatory and anti-inflammatory signaling molecules were calculated and compared between intact (VEH_{PLX}) and microglia-depleted (PLX3397) SCN organotypic explants

Discussion

Results of this study confirm that microglia possess a fully autonomous circadian clock that generates stable oscillations over multiple days in culture. They provide novel evidence that the circadian clock in microglia, as assessed by analysis of bioluminescence rhythms, is modulated according to changes in their polarization. In this respect, their clock behaves similarly as recently described in macrophages (Chen et al. 2020). The results demonstrate that polarization to the pro-inflammatory M1 state decreases the amplitude and shortens the period of the microglial clock, and on the contrary, polarization to the anti-inflammatory phenotype (M2) significantly prolongs the period of the microglial clock. The differences resulted from the effect of polarization on clock genes expression levels. In M1-polarized microglia, mean expression levels of *Cry1* and *Nr1d1* are substantially upregulated. *Cry1* codes protein which plays the role of a negative transcription factor in the TTFL model of the circadian clock, causing repression of the transcriptional activity of CLOCK/BMAL1 complex and subsequent decrease in gene expression, including *Per2*. *Nr1d1* is coding a negative transcriptional factor, which inhibits transcription of *Bmal1*. In accordance, expression levels of *Bmal1* were decreased. Taken together, the M1 polarization-induced modulation of the clock gene expression profiles can explain lower and more rapidly oscillating levels of PER2-driven bioluminescence rhythms that we observed at the cell culture as well as single-cell levels. In M2-polarized microglia, the changes in the molecular clock mechanism, namely increased *Per2* expression in combination with decreased *Bmal1* expression, lead to the opposite result, i.e., bioluminescence rhythms with high amplitude and longer period.

Importantly, the microglial circadian clock flexibly reacts to the changes in the cellular metabolism in response to polarization change. The data presented here provide compelling evidence that the response of microglia's clock to pro-inflammatory stimuli by shortening of the period can be effectively reversed upon subsequent exposure to anti-inflammatory cytokine signals.

Microglia reside within the neural tissue where they actively participate in homeostasis maintenance, ensure neuronal survival, and partake in synaptic plasticity and neurogenesis (Biber et al. 2007; Szepesi et al. 2018; Ronzano et al. 2021). Previously, results of in vivo studies showed disrupted circadian rhythms following microglia elimination in rat SCN and hippocampi (Sominsky et al. 2021), as well as the affected amplitude of circadian rhythms in zebrafish (Mosser et al. 2019). On the other hand, microglia depletion did not affect circadian rhythms in the murine cortex (Barahona et al. 2022). Results of this in vitro study show that microglia depletion in the SCN organotypic explants through CSF-1R inhibition has a significant impact on the robustness of the clock, because it causes a faster decrease in oscillations' amplitude. Microglia depletion did not decrease the viability of the explanted neuronal tissue, which was consistent with previous observations (Ji et al. 2013; Araki et al. 2020).

The main role of microglia is to mediate the inflammatory reaction. The immune reaction is a complex process accompanied by cytokine signaling between microglia and other glial cells, importantly astrocytes. Microglia–astrocyte interaction is maintained via heterogeneous pathways employing neurotransmitters, cytokines, chemokines, NO, ROS, ATP, or glutamate (Matejuk and Ransohoff 2020). In the case of brain insult, as the first line of defense, microglia are activated to secrete an array of cytokines, including IL-1, IL-6, TNFα, or IFNγ, which then trigger the activation of astrocytes (Röhl et al. 2007; Gao et al. 2013). Astrocytes are involved in TNFα-induced modulation of the SCN clock (Duhart et al. 2013). Therefore, in theory, they may be the mediators responsible for the period change of SCN rhythms that we observed in vitro. Murine astrocytes themselves express TLR-4 and respond to LPS stimulation by increased pro-inflammatory cytokine release (Tarassishin et al. 2014). LPS have been previously shown to downregulate clock gene expression in the SCN in vivo. Interestingly, this downregulation has been reported to pass on the second day after LPS stimulation (Okada et al. 2008). It has been demonstrated that around this time (approximately 36 h after LPS stimulation), activated microglia initiate expression of IL-10 anti-inflammatory cytokine (Chhor et al. 2013). This cytokine induces the M2 polarization of microglia (Durafourt et al. 2012; Cherry et al. 2014; Hu et al. 2014; Orihuela et al. 2016) and promotes inflammation suppression through

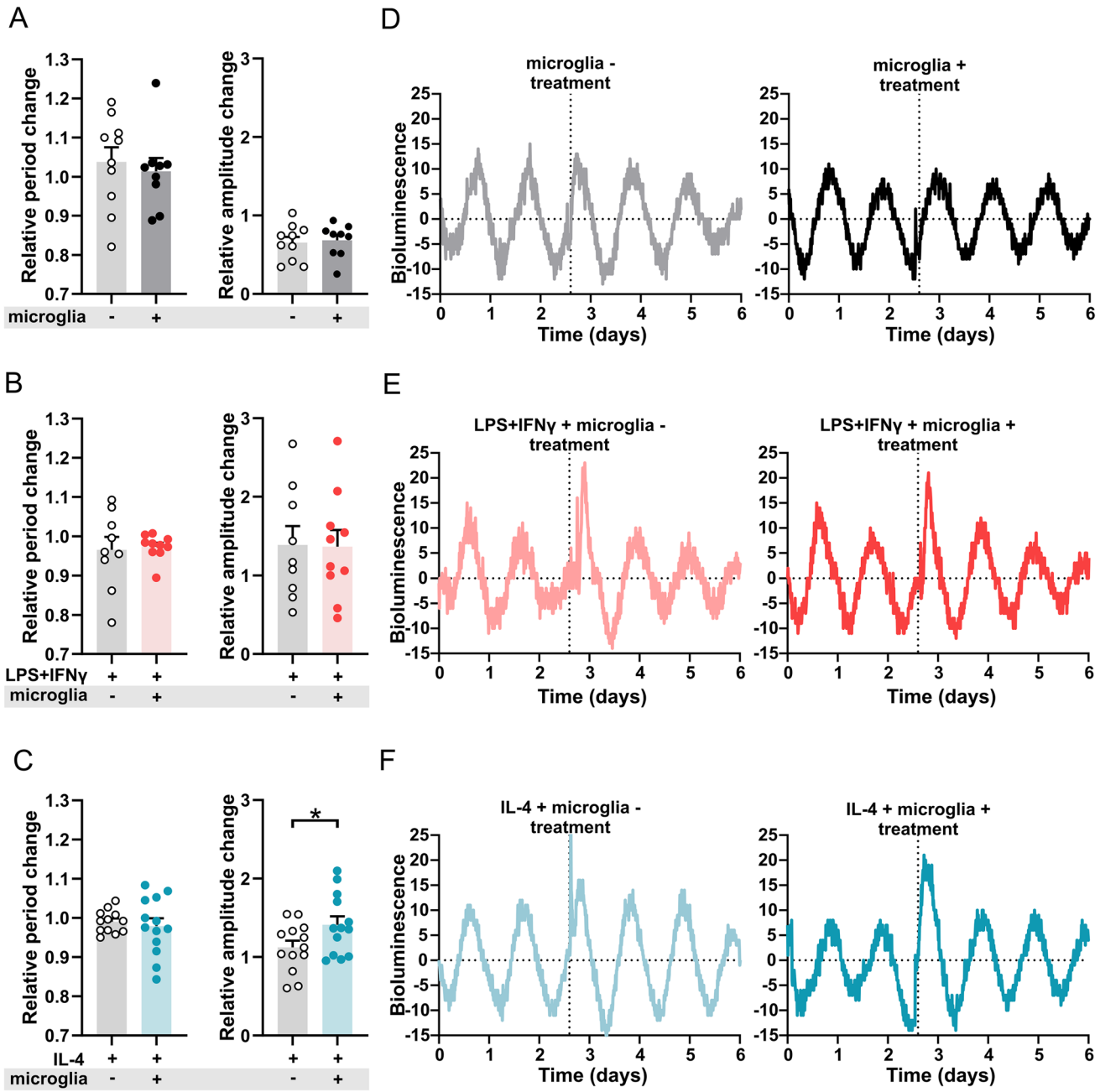

Fig.6 Co-cultivation of microglia-depleted SCN explants with polarized microglia. PLX3397-treated SCN organotypic explants were recorded for two full circadian cycles. After this time, suspension consisting of recording medium and M1- or M2-polarizing molecules (LPS and IFNγ or IL-4, respectively) was applied with or without microglia, approximately 1500 cells per explant. Relative change of period and amplitude before and after treatment with or without **A** M0 **B** M1- or **C** M2-polarized microglia. **D** Representative bioluminescence recordings of PLX3397-treated SCN before and after treatment without (left, gray line) or with (right, black line) resting microglia, **E** representative bioluminescence recordings of PLX3397-treated SCN before and after treatment without (left, pink line) or with (right, red line) M1 microglia, **F** representative bioluminescence recordings of PLX3397-treated SCN before and after treatment without (left, light blue line) or with (right, blue line) M2 microglia. Data are expressed as mean ± SEM. $^{*}P < 0.05$

feedback communication with astrocytes (Norden et al. 2016). Results of this study show that microglia presence mitigates the long-lasting negative effect of LPS exposure on the amplitude of the SCN clock, in accordance with their essential regulatory role in the inflammation resolution process. Co-cultivation of the SCN explants with M2-polarized microglia was specifically able to improve the amplitude of the SCN clock. These findings revealed that the presence of M2-polarized microglia has a beneficial effect on the SCN clock. Microglia

neuroprotective effects may play a role in this effect, but the underlying mechanism remains to be elucidated.

In conclusion, this study provides new insight into the mutual interaction between the circadian and immune systems within the CNS, namely in the structure harboring the central circadian clock.

Supplementary Information The online version contains supplementary material available at https://doi.org/10.1007/s10571-022-01252-1.

Acknowledgements This work was supported by the Grant Agency of Charles University (project GA UK No. 514219), OPPK BrainView CZ.2.16/3.1.00/21544, and Research Project RV0 67985823. The authors thank Eva Tlusta for technical assistance. We would also like to thank Chun-Xia Yi and Irina Milanova (Amsterdam UMC, Amsterdam, Netherlands) for their support and methodology sharing.

Author Contributions All authors contributed to the study execution. PH and AS contributed to study conception and design. PH and KS contributed to material preparation, data collection, and analysis. PH contributed to the first draft of the manuscript. AS reviewed and commented on the following versions of the manuscript. All authors read and approved the final manuscript.

Funding This work was supported by the Grant Agency of Charles University (project GA UK No. 514219), OPPK BrainView CZ.2.16/3.1.00/21544, and Research Project RV0 67985823.

Data Availability Python scripts used for image adjustment of bioluminescence microscopy recordings and bioluminescence data analyses are available at: https://github.com/clockgene. The datasets generated during and/or analyzed during the current study are available from the corresponding author on request.

Declarations

Conflict of interest The authors declare no conflict of interest.

Ethical Approval The Animal Care and Use Committee of the Institute of Physiology, in agreement with the Animal Protection Law of the Czech Republic as well as European Community Council directives 86/609/EEC, approved all experiments.

References

Araki T, Ikegaya Y, Koyama R (2020) Microglia attenuate the kainic acid-induced death of hippocampal neurons in slice cultures. Neuropsychopharmacol Rep 40:85–91. https://doi.org/10.1002/npr2.12086

Barahona RA, Morabito S, Swarup V, Green KN (2022) Cortical diurnal rhythms remain intact with microglial depletion. Sci Rep 12:1–9. https://doi.org/10.1038/s41598-021-04079-w

Bartness TJ, Song CK, Demas GE (2001) SCN efferents to peripheral tissues: implications for biological rhythms. J Biol Rhythms 16:196–204. https://doi.org/10.1177/074873040101600302

Biber K, Neumann H, Inoue K, Boddeke HWGM (2007) Neuronal 'On' and 'Off' signals control microglia. Trends Neurosci 30:596–602. https://doi.org/10.1016/j.tins.2007.08.007

Blasko I, Stampfer-Kountchev M, Robatscher P et al (2004) How chronic inflammation can affect the brain and support the development of Alzheimer's disease in old age: the role of microglia and astrocytes. Aging Cell 3:169–176. https://doi.org/10.1111/j.1474-9728.2004.00101.x

Bollinger T, Schibler U (2014) Circadian rhythms-From genes to physiology and disease. Swiss Med Wkly. https://doi.org/10.4414/smw.2014.13984

Bollinger T, Leutz A, Leliavski A et al (2011) Circadian clocks in mouse and human CD4+ T cells. PLoS ONE 6:e29801. https://doi.org/10.1371/journal.pone.0029801

Chen S, Fuller KK, Dunlap JC, Loros JJ (2020) A pro- and anti-inflammatory axis modulates the macrophage circadian clock. Front Immunol 11:867. https://doi.org/10.3389/fimmu.2020.00867

Cherry JD, Olschowka JA, O'Banion M (2014) Neuroinflammation and M2 microglia: the good, the bad, and the inflamed. J Neuroinflammation 11:98. https://doi.org/10.1186/1742-2094-11-98

Chhor V, Le Charpentier T, Lebon S et al (2013) Characterization of phenotype markers and neuronotoxic potential of polarised primary microglia in vitro. Brain Behav Immun 32:70–85. https://doi.org/10.1016/j.bbi.2013.02.005

Chi-Castañeda D, Ortega A (2016) Clock genes in glia cells. ASN Neuro 8:175909141667076. https://doi.org/10.1177/1759091416670766

Coleman LG, Zou J, Crews FT (2020) Microglial depletion and repopulation in brain slice culture normalizes sensitized proinflammatory signaling. J Neuroinflammation 17:27. https://doi.org/10.1186/s12974-019-1678-y

Cui L, Jin X, Xu F et al (2021) Circadian rhythm-associated Rev-erbα modulates polarization of decidual macrophage via the PI3K/Akt signaling pathway. Am J Reprod Immunol. https://doi.org/10.1111/aji.13436

Davalos D, Grutzendler J, Yang G et al (2005) ATP mediates rapid microglial response to local brain injury in vivo. Nat Neurosci 8:752–758. https://doi.org/10.1038/nn1472

Duhart JM, Leone MJ, Paladino N et al (2013) Suprachiasmatic astrocytes modulate the circadian clock in response to TNF-. J Immunol 191:4656–4664. https://doi.org/10.4049/jimmunol.1300450

Durafourt BA, Moore CS, Zammit DA et al (2012) Comparison of polarization properties of human adult microglia and blood-derived macrophages. Glia 60:717–727. https://doi.org/10.1002/glia.22298

Fonken LK, Frank MG, Kitt MM et al (2015) Microglia inflammatory responses are controlled by an intrinsic circadian clock. Brain Behav Immun 45:171–179. https://doi.org/10.1016/j.bbi.2014.11.009

Gao Z, Zhu Q, Zhang Y et al (2013) Reciprocal modulation between microglia and astrocyte in reactive gliosis following the CNS injury. Mol Neurobiol 48:690–701. https://doi.org/10.1007/s12035-013-8460-4

Greenhalgh AD, David S (2014) Differences in the phagocytic response of microglia and peripheral macrophages after spinal cord injury and its effects on cell death. J Neurosci 34:6316–6322. https://doi.org/10.1523/JNEUROSCI.4912-13.2014

Greter M, Merad M (2013) Regulation of microglia development and homeostasis. Glia 61:121–127. https://doi.org/10.1002/glia.22408

Güldner FH (1983) Numbers of neurons and astroglial cells in the suprachiasmatic nucleus of male and female rats. Exp Brain Res 50:373–376. https://doi.org/10.1007/BF00239203

Hayashi Y (2013) Diurnal spatial rearrangement of microglial processes through the rhythmic expression of P2Y12 receptors. J Neurol Disord 01:1–7. https://doi.org/10.4172/2329-6895.1000120

Hu X, Leak RK, Shi Y et al (2014) Microglial and macrophage polarization—new prospects for brain repair. Nat Rev Neurol 11:56–64. https://doi.org/10.1038/nrneurol.2014.207

Ji K, Akgul G, Wollmuth LP, Tsirka SE (2013) Microglia actively regulate the number of functional synapses. PLoS ONE 8:e56293. https://doi.org/10.1371/journal.pone.0056293

Kabba JA, Xu Y, Christian H et al (2018) Microglia: housekeeper of the central nervous system. Cell Mol Neurobiol 38:53–71. https://doi.org/10.1007/s10571-017-0504-2

Kawai M, Rosen CJ (2010) PPARγ: a circadian transcription factor in adipogenesis and osteogenesis. Nat Rev Endocrinol 6:629–636. https://doi.org/10.1038/nrendo.2010.155

Kettenmann H, Hoppe D, Gottmann K et al (1990) Cultured microglial cells have a distinct pattern of membrane channels different from peritoneal macrophages. J Neurosci Res 26:278–287. https://doi.org/10.1002/jnr.490260303

Lawson LJ, Perry VH, Gordon S (1992) Turnover of resident microglia in the normal adult mouse brain. Neuroscience 48:405–415. https://doi.org/10.1016/0306-4522(92)90500-2

Li Y, Yang Y-Y, Ren J-L et al (2017) Exosomes secreted by stem cells from human exfoliated deciduous teeth contribute to functional recovery after traumatic brain injury by shifting microglia M1/M2 polarization in rats. Stem Cell Res Ther 8:198. https://doi.org/10.1186/s13287-017-0648-5

Li Y, Shan Y, Desai RV et al (2020) Noise-driven cellular heterogeneity in circadian periodicity. Proc Natl Acad Sci 117:10350–10356. https://doi.org/10.1073/pnas.1922388117

Martínez-Tapia RJ, Chavarría A, Navarro L (2020) Differences in diurnal variation of immune responses in microglia and macrophages: review and perspectives. Cell Mol Neurobiol 40:301–309. https://doi.org/10.1007/s10571-019-00736-x

Matejuk A, Ransohoff RM (2020) Crosstalk between astrocytes and microglia: an overview. Front Immunol. https://doi.org/10.3389/fimmu.2020.01416

Mosser EA, Chiu CN, Tamai TK et al (2019) Identification of pathways that regulate circadian rhythms using a larval zebrafish small molecule screen. Sci Rep 9:12405. https://doi.org/10.1038/s41598-019-48914-7

Nakazato R, Hotta S, Yamada D et al (2017) The intrinsic microglial clock system regulates interleukin-6 expression. Glia 65:198–208. https://doi.org/10.1002/glia.23087

Norden DM, Trojanowski PJ, Walker FR, Godbout JP (2016) Insensitivity of astrocytes to interleukin 10 signaling following peripheral immune challenge results in prolonged microglial activation in the aged brain. Neurobiol Aging 44:22–41. https://doi.org/10.1016/j.neurobiolaging.2016.04.014

Novosadová Z, Polidarová L, Sládek M, Sumová A (2018) Alteration in glucose homeostasis and persistence of the pancreatic clock in aged mPer2Luc mice. Sci Rep 8:11668. https://doi.org/10.1038/s41598-018-30225-y

Okada K, Yano M, Doki Y et al (2008) Injection of LPS causes transient suppression of biological clock genes in rats. J Surg Res 145:5–12. https://doi.org/10.1016/j.jss.2007.01.010

Orihuela R, McPherson CA, Harry GJ (2016) Microglial M1/M2 polarization and metabolic states. Br J Pharmacol 173:649–665. https://doi.org/10.1111/bph.13139

Oster H, Damerow S, Kiessling S et al (2006) The circadian rhythm of glucocorticoids is regulated by a gating mechanism residing in the adrenal cortical clock. Cell Metab 4:163–173. https://doi.org/10.1016/j.cmet.2006.07.002

Partch CL, Green CB, Takahashi JS (2014) Molecular architecture of the mammalian circadian clock. Trends Cell Biol 24:90–99. https://doi.org/10.1016/j.tcb.2013.07.002

Peferoen L, Kipp M, van der Valk P et al (2014) Oligodendrocyte-microglia cross-talk in the central nervous system. Immunology 141:302–313. https://doi.org/10.1111/imm.12163

Pevet P, Challet E (2011) Melatonin: both master clock output and internal time-giver in the circadian clocks network. J Physiol 105:170–182. https://doi.org/10.1016/j.jphysparis.2011.07.001

Prinz M, Priller J (2014) Microglia and brain macrophages in the molecular age: from origin to neuropsychiatric disease. Nat Rev Neurosci 15:300–312. https://doi.org/10.1038/nrn3722

Prolo LM, Takahashi JS, Herzog ED (2005) Circadian rhythm generation and entrainment in astrocytes. J Neurosci 25:404–408. https://doi.org/10.1523/JNEUROSCI.4133-04.2005

Rampersad SN (2012) Multiple applications of alamar blue as an indicator of metabolic function and cellular health in cell viability bioassays. Sensors 12:12347–12360. https://doi.org/10.3390/s120912347

Röhl C, Lucius R, Sievers J (2007) The effect of activated microglia on astrogliosis parameters in astrocyte cultures. Brain Res 1129:43–52. https://doi.org/10.1016/j.brainres.2006.10.057

Ronzano R, Roux T, Thetiot M et al (2021) Microglia-neuron interaction at nodes of Ranvier depends on neuronal activity through potassium release and contributes to remyelination. Nat Commun 12:5219. https://doi.org/10.1038/s41467-021-25486-7

Scheiermann C, Kunisaki Y, Frenette PS (2013) Circadian control of the immune system. Nat Rev Immunol 13:190–198. https://doi.org/10.1038/nri3386

Schindelin J, Arganda-Carreras I, Frise E et al (2012) Fiji: an open-source platform for biological-image analysis. Nat Methods 9:676–682. https://doi.org/10.1038/nmeth.2019

Silver AC, Arjona A, Hughes ME et al (2012) Circadian expression of clock genes in mouse macrophages, dendritic cells, and B cells. Brain Behav Immun 26:407–413. https://doi.org/10.1016/j.bbi.2011.10.001

Sládek M, Sumová A (2019) Modulation of NMDA-mediated clock resetting in the suprachiasmatic nuclei of mPer2Luc mouse by endocannabinoids. Front Physiol. https://doi.org/10.3389/fphys.2019.00361

Sládek M, Polidarová L, Nováková M et al (2012) Early chronotype and tissue-specific alterations of circadian clock function in spontaneously hypertensive rats. PLoS ONE 7:e46951. https://doi.org/10.1371/journal.pone.0046951

Sominsky L, Dangel T, Malik S et al (2021) Microglial ablation in rats disrupts the circadian system. FASEB J. https://doi.org/10.1096/fj.202001555RR

Son GH, Chung S, Choe HK et al (2008) Adrenal peripheral clock controls the autonomous circadian rhythm of glucocorticoid by causing rhythmic steroid production. Proc Natl Acad Sci U S A 105:20970–20975. https://doi.org/10.1073/pnas.0806962106

Szepesi Z, Manouchehrian O, Bachiller S, Deierborg T (2018) Bidirectional microglia-neuron communication in health and disease. Front Cell Neurosci. https://doi.org/10.3389/fncel.2018.00323

Takahashi K, Yamamura F, Naito M (1989) Differentiation, maturation, and proliferation of macrophages in the mouse yolk sac: a light-microscopic, enzyme-cytochemical, immunohistochemical, and ultrastructural study. J Leukoc Biol 45:87–96. https://doi.org/10.1002/jlb.45.2.87

Tang Y, Le W (2016) Differential roles of M1 and M2 microglia in neurodegenerative diseases. Mol Neurobiol 53:1181–1194. https://doi.org/10.1007/s12035-014-9070-5

Tarassishin L, Suh HS, Lee SC (2014) LPS and IL-1 differentially activate mouse and human astrocytes: Role of CD14. Glia 62:999–1013. https://doi.org/10.1002/glia.22657

Timmons GA, O'Siorain JR, Kennedy OD et al (2020) Innate rhythms: clocks at the center of monocyte and macrophage function. Front Immunol. https://doi.org/10.3389/fimmu.2020.01743

Tinevez J-Y, Perry N, Schindelin J et al (2017) TrackMate: an open and extensible platform for single-particle tracking. Methods 115:80–90. https://doi.org/10.1016/j.ymeth.2016.09.016

Tomida M, Yamamoto-Yamaguchi Y, Hozumi M (1984) Purification of a factor inducing differentiation of mouse myeloid leukemic M1 cells from conditioned medium of mouse fibroblast L929 cells. J Biol Chem 259:10978–10982

Wang X-L, Wolff SEC, Korpel N et al (2020) Deficiency of the circadian clock gene Bmal1 reduces microglial immunometabolism. Front Immunol. https://doi.org/10.3389/fimmu.2020.586399

Wen L, You W, Wang H et al (2018) Polarization of microglia to the M2 phenotype in a peroxisome proliferator-activated receptor gamma-dependent manner attenuates axonal injury induced by traumatic brain injury in mice. J Neurotrauma 35:2330–2340. https://doi.org/10.1089/neu.2017.5540

Yamamoto T, Nakahata Y, Tanaka M et al (2005) Acute physical stress elevates mouse period1 mRNA expression in mouse peripheral tissues via a glucocorticoid-responsive element. J Biol Chem 280:42036–42043. https://doi.org/10.1074/jbc.M509600200

Yamazaki S, Takahashi JS (2005) In real-time luminescence reporting of circadian gene expression in mammals. Methods Enzymol 393:288–301

Yoo S-H, Yamazaki S, Lowrey PL et al (2004) PERIOD2::LUCIFERASE real-time reporting of circadian dynamics reveals persistent circadian oscillations in mouse peripheral tissues. Proc Natl Acad Sci 101:5339–5346. https://doi.org/10.1073/pnas.0308709101